Hindawi
Journal of Sensors
Volume 2022, Article ID 6988001, 12 pages
https://doi.org/10.1155/2022/6988001

Research Article

Design of Health Detection System for Elderly Smart Watch Based on Biosignal Acquisition

Zhu Zhu,[1] **Peixian Wang**,[2] **and Fuguang Wang**[3]

[1]*College of Art, Shangqiu University, Shangqiu, Henan 476000, China*
[2]*College of Art, Sangmyung University, Cheonan 31066, Republic of Korea*
[3]*Mechanical and Electrical Engineering Department, Liaocheng Vocational and Technical College, Liaocheng, Shandong 252000, China*

Correspondence should be addressed to Zhu Zhu; 14058@sqxy.edu.cn

Received 28 May 2022; Revised 6 July 2022; Accepted 9 July 2022; Published 30 July 2022

Academic Editor: Gengxin Sun

The health monitoring of the elderly has attracted increasing attention of researchers. Based on the biosignal acquisition method, this paper proposes a design structure of the health detection system for smart watches for the elderly and realizes the effective detection of health signals by analyzing the Lipschitz exponent of the maximum value column of the transform. The multiphysiological parameter acquisition and monitoring system of the wearable smart watch designed in this paper can continuously monitor the physiological parameters of the elderly such as body temperature, pulse, and respiration for a long time and solve the problem of the accuracy of the health detection of the elderly. In the simulation process, based on the performance of the synchronization source and the difference of the network path, the model applies the multivariate and multiscale biological signals to collect the human gait acceleration. The experimental results show that, compared with the international recognition rate obtained for this data set, the highest recognition rate obtained by the method in this paper reaches 96.5%, which can provide a calibration accuracy of 1 ~ 50 ms, and the synchronized system time and the national time service center network are given. The error obtained by comparing the published time is within 50 ms, which meets the accuracy requirements of the time protocol. The results fully prove that the algorithm in this paper can effectively extract the biosignal features of the elderly's health detection and has good statistical features and classification accuracy.

1. Introduction

With the intensification of aging social problems, the health problems of middle-aged and elderly people have increasingly attracted people's attention [1]. Therefore, real-time monitoring of physiological signals such as daily exercise posture and heart rate of middle-aged and elderly people, and assessment of the physical health of middle-aged and elderly people, has important social significance [2]. Wearable devices have the advantages of small size and easy portability and can realize the dynamic acquisition of human physiological signals under low physiological and psychological pressure [3], which is of great practicality for the daily health monitoring of the middle-aged and the elderly and the rehabilitation of patients [4]. The combination of wearable devices and medical and health fields will become an important health-monitoring device under the new medical model. There is no doubt that mobile medical care is bound to be the future trend [5].

With the rapid development of network technology in recent years, the network of community care has become a trend [6]. Using the Internet for community medical care can on the one hand strengthen information sharing with large medical institutions such as hospitals [7–9]; the network monitoring system generally adopts the form of server/client [10]. The client mainly carries out the collection and preliminary processing of physiological information; the server mainly carries out data collection and subsequent processing; the client and the server carry out data exchange through the network [11]. It is of great practical significance to actively improve and maintain the health of the elderly, improve the health quality of the people,

prolong the healthy life expectancy of the people, ensure the sustainable development of the social economy, promote the harmonious progress between man and nature [12], and improve the health literacy and quality of life of the elderly. Therefore, it is necessary to carry out health management work for the elderly, to do a good job in the prevention and treatment of chronic diseases, and to improve their health level [13–15].

This design applies the mainstream microprocessors, sensors, and wireless communication technologies on the market, as well as the specific health conditions of the elderly, to design a practical and stable low-power wearable smart watch elderly health monitoring system, use temperature sensors and pulse sensors to collect human physiological parameters, and then use low-power smart watch technology for data transmission, using smart watches with a high market share as terminals to collect and display body temperature, pulse, posture, and other physiological parameters. Through this system, the physical condition of the elderly can be found in time, and the system can also realize real-time monitoring and remote monitoring of the physiological parameters of the human body through various sensors. The main work of this paper is to use green light as the light source for heart rate detection to reduce the impact on the heart rate detection results caused by changes in blood flow at the wrist: during waveform preprocessing, a Butterworth low-pass filter is used to smooth the waveform; in biological signal detection, the idea of the K-means clustering algorithm is used for reference, and a hierarchical screening algorithm is used for biological signal detection, thereby ensuring the accuracy of the heart rate detection algorithm.

2. Related Work

In the face of behavioral state perception and physiological multisource heterogeneous data aggregation, transmission communication, and processing computing requirements, we need to further develop new low-power and stable and reliable communication network and transmission network architecture [16]. The system collects the patient's biological signals through sensors and sends the signals to the monitoring center through GPRS. The monitoring center automatically recognizes, records, and analyzes biological signals and automatically alarms according to the analysis results. The development and introduction of wireless short-distance data transmission technology that has made the application of wearable computing have a broader development space [17].

Sundaravadivel et al. [18] use a reflective photoelectric detection device composed of an LED light source with a wavelength of 660 nm and a photodetector to obtain the PPG signal in the arterial blood and analyze the frequency domain characteristics by performing fast Fourier transform on the obtained PPG signal, so as to achieve detection of human heart rate. Tamiziniyan and Keerthana [19] proposed a method that combines PPG technology and image-based noncontact heart rate detection. The color video of the face is obtained through the camera, the video is converted into a digital signal through a digital image processing method, and then the PPG is obtained through blind source separation.

Lee et al. [20] proposed a method for measuring heart rate using facial video, and under natural light conditions, a common camera and blind source separation method were used to measure human heart rate. This method is an earlier proposed video-based heart rate detection method. Cho et al. [21] proposed a video-based method for heart rate detection. The method uses the smart watch camera to collect video, uses the face recognition algorithm to extract the effective area in the video information of the face collected by the smart watch camera, calculates the pixel average value of the signals in the area according to the three RGB channels, then standardizes the pixel mean value, and then detects the peaks of the time-domain frequency band, so as to obtain the method of calculating the heart rate using the smart watch. This method is easily affected by factors such as ambient light interference and the stability of the detector's posture; so, the quality of the collected signal affects the estimation result, thereby affecting the accuracy of the heart rate detection result. Mardini et al. [22] used a supervised learning multilayer neural network model for heart rate estimation. The method is to use the acceleration sensor and GPS sensor in the smart watch to collect line data for testing. This method is combined with aerobic exercise for heart rate detection and calculation. The input of the algorithm is the acceleration horizontal component, vertical component, route gradient, and oxygen consumption, and the heart rate calculation result is the output. The evaluation results show that the heart rate value detected by this method is basically consistent with the human heart rate variability in a resting state, but the learning ability of this method for heart rate variability needs to be strengthened [23, 24].

3. Design of Health Detection System Based on Biological Signal Acquisition

3.1. Biosignal Acquisition Topology. The design of the biological signal acquisition system is based on the LPC1769 microprocessor and uses the HK-2000 pressure sensor, DS18B20 temperature sensor, MMA7455 sensor, and smart watch module. The signal collected by the sensor is processed by the amplifying circuit and the compensation circuit, converted into a digital signal by AD, and finally judged by the program to realize the monitoring process to the preset smart watch. This set of elderly monitoring system can realize body temperature detection, pulse detection, and judgment of health and can transmit human physiological data to the host computer through smart watches. At the same time, the preset smart watch can also call up the elderly's physiological constants, geographic location, historical records, and other information at any time through text messages.

$$x(s,t) = \left\{(i(s),\nabla t), \left(i^2(s),\nabla t\right), \left(i^3(s),\nabla t\right), \cdots, \left(i^n(s),\nabla t\right)\right\},$$

$$\sum \operatorname{cov}(k,k-1) + \operatorname{cov}(i,j) > \sum \operatorname{cov}(k-1,k) + \operatorname{cov}(i-k,j-k) > 1. \tag{1}$$

The analysis shows that the SMVW of static and normal walking is not large, and the maximum value is about 1.2 rad/s. The SMVW of running and jumping is slightly changed than that of static and normal walking, but the maximum value is about 1.8 rad/s. SMVW will change greatly when healthy, and the maximum value of SMVW when healthy is about 7 rad/s.

Because of the large number of mathematical formulas involved in the LADT algorithm, the program does not use the advanced Simulink development environment but is mainly implemented through M-files, and then the program is packaged into a Simulink model. According to the experimental results, the threshold SMVWT of SMVW can be set as 2 rad/s.

It can write the programs shown in Figure 1 in assembly language, *C* language, or a mixture of assembly language and *C* language, then convert them into DSP assembly language, and send them to the compiler for compilation to generate object files (*.obj). Send the object file to the linker for linking and get the executable code file (*.out). Download the executable code file to the debugger for online running and debugging and check whether the running result is correct. The data collected by various sensors is coordinated and summarized, the received data is filtered, stored, and analyzed through microprocessing, and the analyzed data saves and transmits the physical condition data to the designated upper computer (the old man's mobile terminal) by means of wireless Bluetooth.

$$\begin{pmatrix} \sin p & -1 \\ 1 & \cos p \end{pmatrix} \begin{pmatrix} \frac{1}{p} & -1 \\ 1 & -\frac{1}{p} \end{pmatrix} = \begin{pmatrix} \frac{1}{p} & -\cos k \\ \sin k & -\frac{1}{p} \end{pmatrix},$$
$$\begin{cases} \text{hrest}(x, y) = \text{median}(q(r-1), p(r-1)), \\ \text{teration}(q, p) > 1. \end{cases} \tag{2}$$

When judging acceleration and angular velocity, it is only necessary to calculate SMVA and SMVW, and it is not necessary to judge the spatial direction of acceleration and angular velocity. This is because no matter which direction the human body is healthy, it will lead to the instantaneous change of SVMA and SVMW, which can be used as one of the thresholds to judge whether health occurs, which can not only greatly reduce the complexity of monitoring but also effectively achieve health detection.

$$\begin{aligned} \text{swma}(x, y) &= \left[\sqrt{a+b} * \sqrt{\ln\,(i + x * j)}\right] * s(x, y), \\ \frac{\text{Uesersw}(x, y)}{U(x, y)} &= \frac{w - b * \ln\,(i + w * j)}{\sqrt{w+b} * \sqrt{\ln\,(i + w * j)}}. \end{aligned} \tag{3}$$

When the body is in a normal state, the collected data is sent to the guardian through the terminal of the elderly and is displayed. In order to ensure comprehensive testing, we divided the volunteers into 8 groups and adopted the simultaneous testing of multiple groups in the same place and the testing of multiple groups at different locations at different times. The first part of the experiment examines the alarm rate of health events. The experiment was carried out by wearing a Hi-watch (Hi-watch A) purchased from the market and then wearing an improved watch (Hi-watch B) with the health detection algorithm written in this article. Forward health, backward health, fall to the left, and health to the right were tested for each experiment. Each volunteer did 10 times for each kind of health, and the total of each kind of health was 100 times.

$$\begin{aligned} &\text{if}(i, j) \longrightarrow \text{delt}(j, i) = |v(1, i) + v(2, i) + \cdots + j(n, i) + (j - n)(n, i)|, \\ &\begin{cases} ds^q(t) - d[m + s]dt = s^q(t) + s^q(t-1), \\ dr^q(t) + d[m + r]dt = r^q(t) - r^q(t-1). \end{cases} \end{aligned} \tag{4}$$

When the PCI bus is operating, the initiator (Master) first sets REQ#, when it gets the permission of the arbiter (GNT#), it will set FRAME# low, and place the Slave address on the AD bus, while #Places command signal indicating the type of transfer to follow. All devices on the PCI bus need to decode this address, and the selected device should set DEVSEL# to declare itself selected. Data can then be transferred when both IRDY# and TRDY# are deasserted.

3.2. Intelligent Data Mining Method. According to the collected relevant health information, the intelligent data evaluation software provided is used to generate the "Elderly Health Risk Evaluation Report" for the elderly by computer: the 5-year incidence risk of major chronic diseases and the lowest risk (or target risk) of the elderly after controlling for risk factors and the average of the same age and gender group risk comparison, while listing the main risk factors associated with the onset of each disease in the elderly and formulating health management prescriptions and health improvement action guidelines for the health risk factors of the elderly.

$$\begin{aligned} &\max\left\{\frac{P(h(a, b) - 1 | v(a, b))}{\sqrt{Ph(a, b) = v(a, b)}}\right\} \\ &\quad < \min\{1, v(a, b)\}, \\ &\lim\left[\frac{y(x, t-1) - dy^q(x - t, t) - dxdy^q(x - t, t)}{y(t, t-1)}\right] - 1 \\ &\quad > 0. \end{aligned} \tag{5}$$

Pulse detection uses (HK-2000) integrated pulse sensor, which uses highly integrated technology to integrate force-sensitive components, temperature-sensing components, and signal conditioning circuits into the sensor. Pulse fluctuations output one positive pulse at a time. The output waveform is shown in it. It takes the pulse signal of the pulse through the inverter to enter the external interrupt of the microcontroller, counts the pulse, and then calculates it within one minute according to the

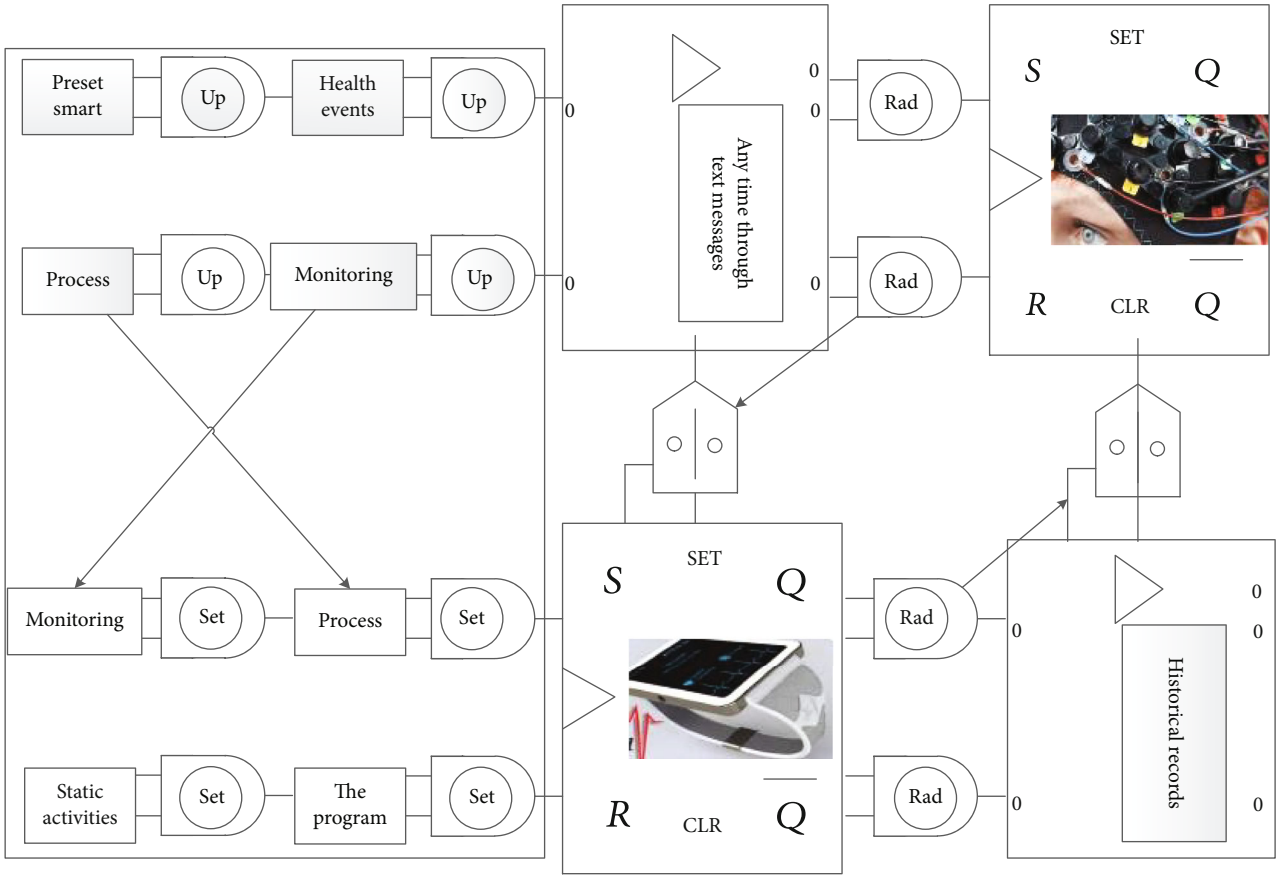

Figure 1: Topological structure of biological signal acquisition.

formula $n = (60^{*}\mathrm{N1}^{*}\mathrm{fs})/N$. Among them, N is the number of sampling, N1 is the number of pulses sampled, and fs is the sampling frequency.

$$\left|\frac{\delta[m(a), m(a-1)]}{m(a) - m(a-1)}\right| + \left|\frac{\delta[k(\mathrm{t}), k(t-1)]}{k(\mathrm{t}) - k(t-1)}\right| + \left|\frac{\delta[g(\mathrm{t}), g(t-1)]}{g(\mathrm{t}) - g(t-1)}\right| = 1,$$

$$\sum \mathrm{pert}(i-k, j-k) < \sum \mathrm{pert}(k, k-1) < \sum \mathrm{pert}(i, j) < \sum \mathrm{pert}(k-1, k). \tag{6}$$

We establish a space rectangular coordinate system for the human body, the human body stands vertically, take the normal direction of the coronal plane of the human body backward as the positive direction of the z-axis of the MMA7455 chip, the normal direction of the sagittal plane to the right is the positive direction of the x-axis of the MMA7455 chip, and the normal direction of the horizontal plane is upward. It is the positive direction of the y-axis of the MMA7455 chip. At this time, the direction of the y-axis is opposite to the direction of the gravitational acceleration g. When the accelerometer is worn at the position of the human lumbar spine, its three sensitive directions are, respectively, consistent with the three axes of the human coordinate system.

It is mainly composed of three parts, namely, the main control module (microprocessing), the sensor module, and the wireless communication module. The body temperature, pulse, and other raw data are obtained through external sensors and then filtered, amplified, and processed. Daily activities such as sitting, lying down, and normal walking belong to the nonvigorous exercise state, while fast walking a nd healthy belong to the strenuous exercise state. When health occurs, the svm increases significantly, typically peaking above 1.5 g (g is the acceleration of gravity) process as shown.

$$\mathrm{uister}(i, i(t)) = \mathrm{imumv}\left\{(u(t), i), \left(u^2(t), i\right), \left(u^3(t), i\right), \cdots, (u^n(t), i)\right\}, \frac{1 - \mathrm{dr}^q(t) - \mathrm{dt} - \mathrm{dW}(t)}{\mathrm{q(t)dt} + \mathrm{dr}^q(t)\mathrm{dW}(t) + \mathrm{q(t-r)dt} + \mathrm{dr}^q(t-r)\mathrm{dW}(t)} \subseteq \mathrm{Sigmer}(r, t). \tag{7}$$

Through the above rough sieve, possible biological signals are screened out. To ensure the accuracy of biological signals, further screening is required. The main basis for

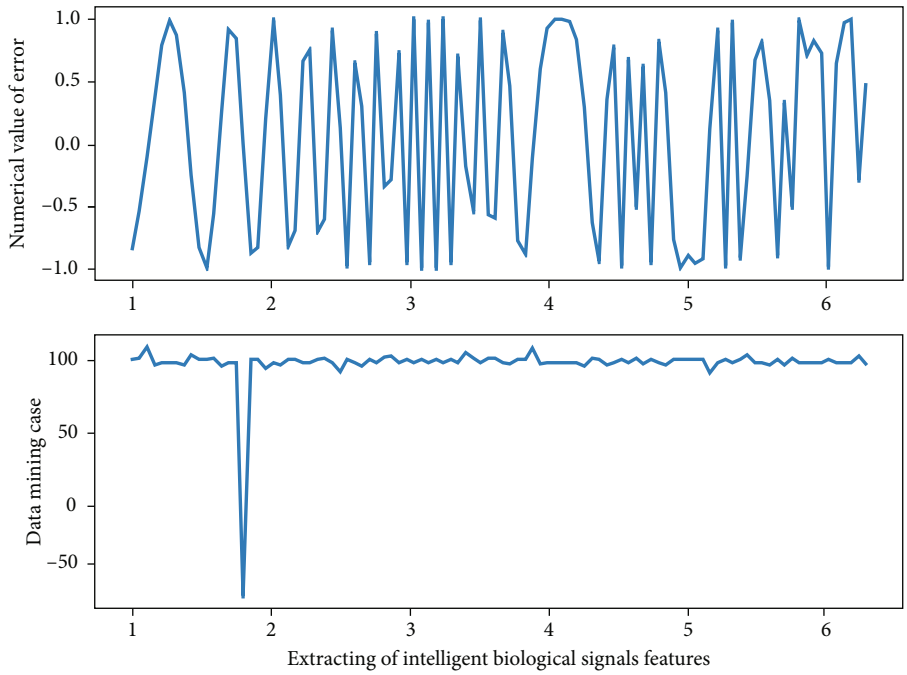

Figure 2: Data mining of intelligent biological signals.

the biosignal screening after the second round is as follows: first, the two adjacent biosignals are separated by a certain distance, not too close; the second is that the width and depth between the two adjacent biosignals will not mutation occurs.

$$\begin{cases} \begin{cases} pb(i) > 1, pb(j) > 1, pb(i+j) > 1 \\ \sqrt{dpb^{q}(k) - d[k + \delta(pb(k))]dk} = 1 \end{cases}, \\ \begin{cases} \min perber(q,p) = \{px(r-1) - py(r-1)\}, \\ \max perber(q,p) = \{px(q \longrightarrow p) - py(q \longrightarrow p)\}. \end{cases} \end{cases} \tag{8}$$

Due to the influence of the falsely detected biological signal in Figure 2, its width is abnormal. If the falsely detected biosignals are eliminated, their widths are normal and then enter the area B to become real biosignals. Region D has a larger width and a smaller depth. If a biological signal appears, it indicates that the signal is not an effective PPG signal. It can be seen from the above analysis that the determination of the boundaries of these four regions affects the accuracy of biological signal detection. Through research, these four regional boundaries will be determined iteratively. Assuming that there are actually biological signals with an average width of Ebb in a PPG signal, all of them are detected in the first screening, and the number of falsely detected biological signals is S.

The elderly terminal of the system in Figure 3 applies cutting-edge technologies such as multichannel sensor integration technology, smart watch communication technology, and multidata fusion technology. It is mainly composed of three parts, namely, the main control module (microprocessing), the sensor module, and the wireless communication module. The raw data such as body temperature and pulse are obtained through external sensors and then filtered, amplified, processed, and then collected through AD to obtain the data of human health. After microprocessing through MCU, the collected data is packaged into it. The data packets are sent to the smart watch side for further processing. After the smart watch terminal receives the data, when the smart watch terminal judges that the received data is abnormal or that the health danger occurs, it will send a short message warning of danger to the preset guardian or doctor through the GSM network.

3.3. Biosignal Data Fitting. The accuracy of the heart rate detection algorithm in this paper, the experiment uses the PM8000-Express pulse oximeter produced by a clinically recognized company for accuracy comparison detection. During the experiment, the heart rate value was measured from the left wrist using the company's product; the heart rate value was measured from the right wrist using the smart watch embedded with the heart rate detection algorithm adopted in this paper.

When the body is in a normal state, the collected data is sent to the guardian through the terminal of the elderly and is displayed. In order to ensure comprehensive testing, we divided the volunteers into 8 groups and adopted the simultaneous testing of multiple groups in the same place and the testing of multiple groups at different locations at different times. At the same time, the data on the effect of health management intervention on blood sugar in diabetic patients in this study were included in the meta-analysis as unpublished literature, and the glycated hemoglobin (HbAlc) of the health management group relative to the control group was finally obtained through the heterogeneity test and the random effect model. The reduction was 0.99 (0.40, 1.58) (part of the detection index was fasting blood sugar, which

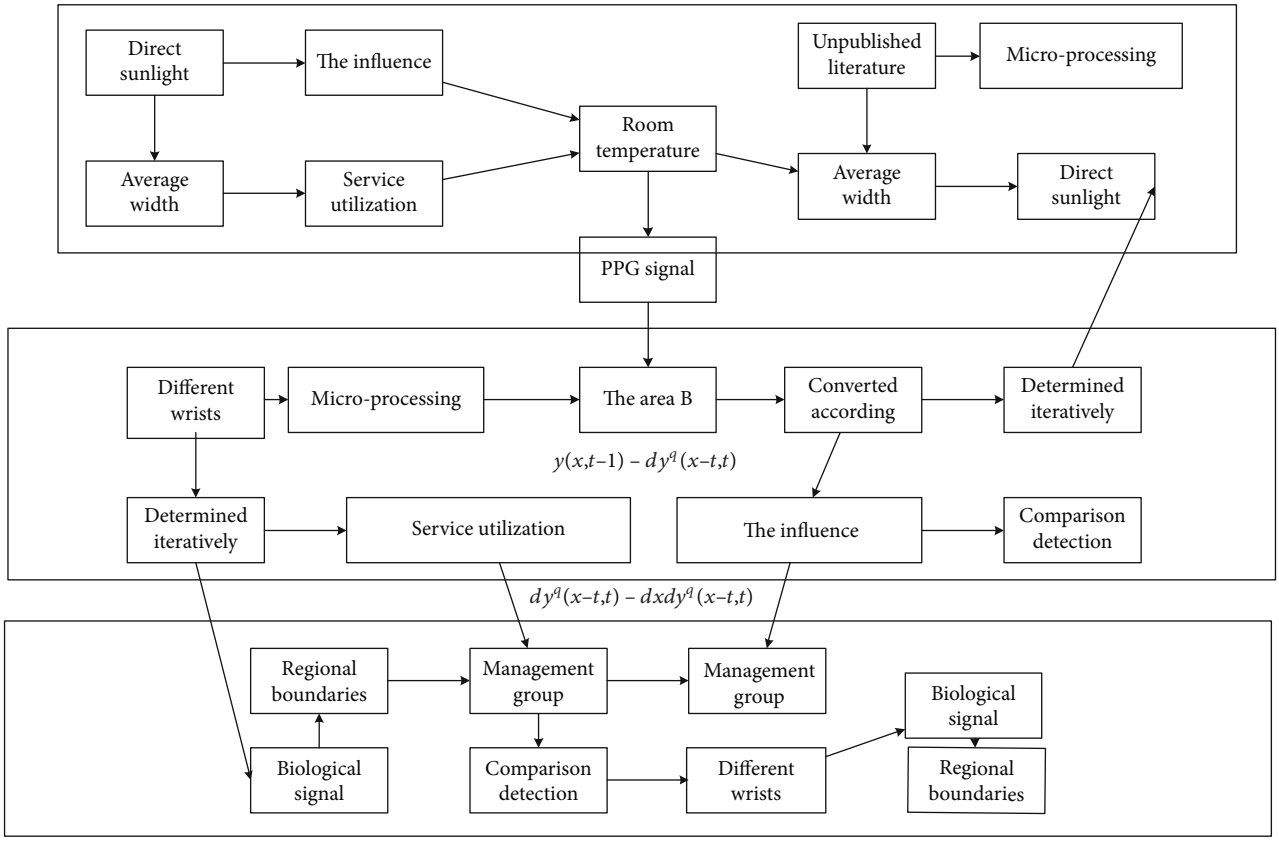

Figure 3: Intelligent data mining sensor integration.

Table 1: Description of biosignal data.

Biosignal case	Sample number	HbAlc value	Reduction rate	Meta value
Method 1	10	11.77	0.40	0.94
Method 2	20	32.08	0.04	0.81
Method 3	30	48.34	0.82	0.04
Method 4	40	39.40	0.38	0.60
Method 5	50	46.61	0.30	0.23
Method 6	60	44.54	0.29	0.16
Method 7	70	28.23	0.23	0.83

was converted according to Table 1), and the average blood sugar is (1.5944 HbAlc-2.5944).

The management group and the control group were compared with multiple indicators such as health knowledge scores, self-assessed health status, health behaviors, related physiological indicators, and health service utilization at baseline. First, the normality test of the data was carried out. For the measurement data indicators, the nonparametric test Mann–Whitney U method was used to compare the management group and the control group. The results showed that except for mild physical activity, female body mass index, and diastolic blood pressure, there was no significant difference in other indicators ($P > 0.05$).

The mean absolute value amplitude of the SEMG signal obtained from the health detection and the coefficients of the 4th-order AR model have shown unparalleled feature representation performance. At the same time, in the real-time SLR system, the feature extraction algorithm has a simple structure, low computational resource overhead, and stable feature expression performance. For the 13 types of detection indicators, we still extract the MAV and 4th-order AR model coefficient features of each channel in the sign language gesture action recognition based on the phonetic code and the head and tail part code. After the program starts, choose your character and choose your current character, which includes an old man, a doctor, and a family member. Next, bind the phone, enter your name and contact number, and then select your relationship with the elderly, whether it is a family member or a doctor. The relationship selected by users of different roles is different.

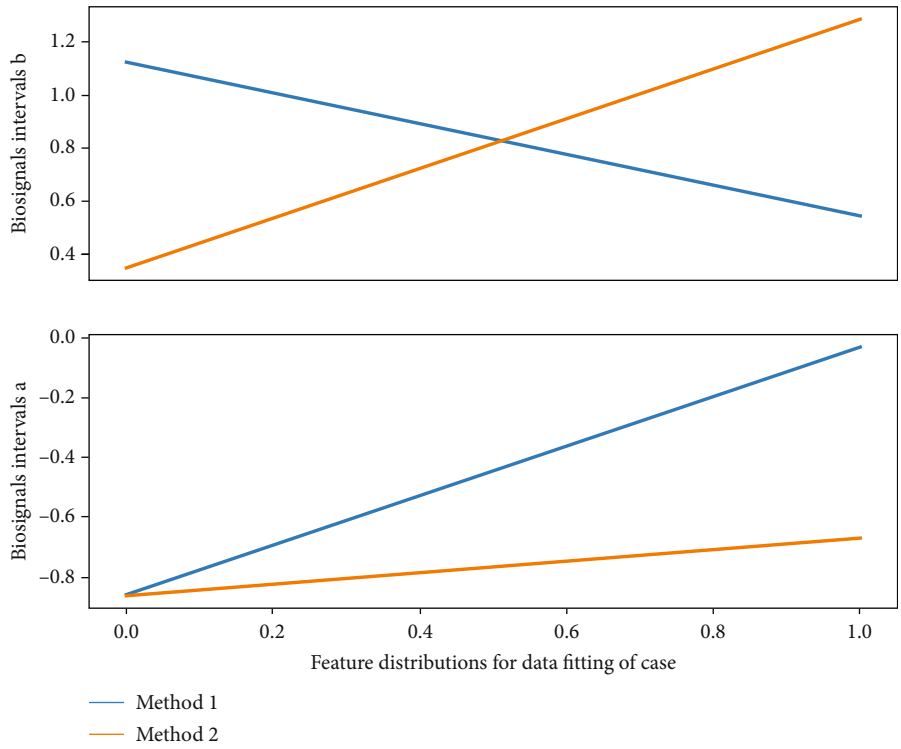

Figure 4: Fitting feature distribution of biosignal data.

3.4. Analysis of Health Test Results. There were 1163 people in the management group and 1198 people in the control group who completed the baseline questionnaire in the health inspection study. There were 957 people in the management group and 1,005 people in the control group who completed both the baseline and the second questionnaire after 18 months. 206 people in the management group were lost to follow-up, with a loss rate of 17.7%; 193 people in the control group were lost to follow-up, with a loss rate of 16.1%. Statistical methods such as *t*-test, chi-square test, and nonparametric test were used to compare the changes of health-related measurement indicators in the management group and the control group before and after 18 months. It is concluded that the utility value of the 50 people in the management group in this study is 0.6623, the standard deviation is 0.2335, the median is 0.7437, the minimum value is 0.1675, the maximum value is 0.9188, and 78% of the respondents have a utility value of 0.2335 and above, 60% at 0.70 and above.

The second part conducts the stability test of the heart rate detection algorithm of Figure 4. The stability comparison experiment is carried out through the smart watch Hi-watch A with its own heart rate detection algorithm and the smart watch Hi-watch B embedded with the heart rate detection algorithm in this paper. Each volunteer used a Hi-watch smart watch with its own algorithm embedded with the algorithm in this paper to perform 10 heart rate detections in a stationary state. According to the change of body posture in health relative to normal behaviors, a health detection algorithm based on body posture information is proposed, and at the same time, the advantages of accelerometers and gyroscopes placed on the chest and thighs of individuals to characterize body posture characteristics are fully utilized. Health detection is successfully implemented, increasing the average recognition rate of actions to 92% while reducing the probability of fall false alarms.

In this paper, because the recognition of the motion trajectory does not need to give the judgment result directly, it needs to be judged together with the likelihood probability of hand shape recognition in Figure 5. Therefore, it is necessary to estimate the likelihood probability of the minimum path cost function here. Similarly, we use the LDC algorithm to model the Gaussian distribution of the probability density within the class, and the feature vector input of the LDC classifier is the path cost function value calculated from a certain type of motion trajectory to all other categories of motion trajectories. Here, only the HMMs of the single-stream SEMG signal are used for detection index pattern recognition. For the specific algorithm, please refer to the previous chapter.

The system can judge the fall of the elderly and perform body temperature detection, pulse detection, and transmit various physiological constants through the Bluetooth module. At the same time, the preset mobile phone (slave machine) can also retrieve the elderly's physiological constants, geographical location, historical records, and other information at any time through SMS. The criterion for judging a certain type of detection index is also modified accordingly to the detection index category corresponding to the HMMs that are most likely to be identified as the HMMs that can generate the maximum likelihood probability.

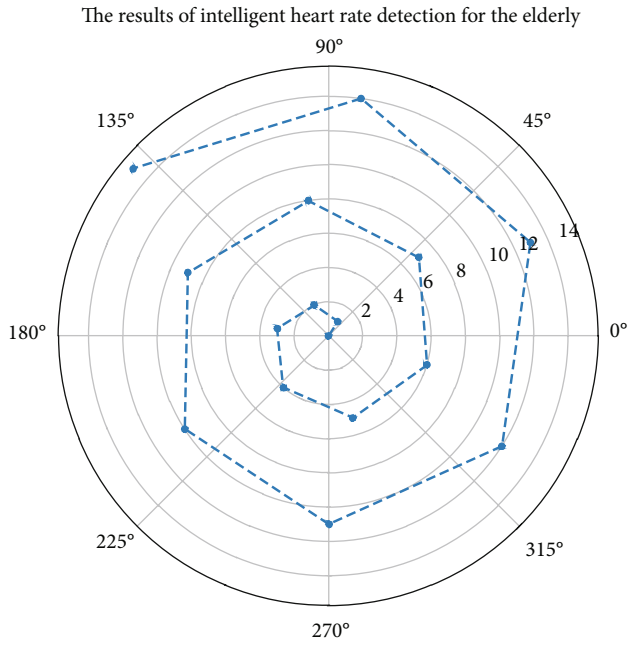

Figure 5: The results of intelligent heart rate detection for the elderly.

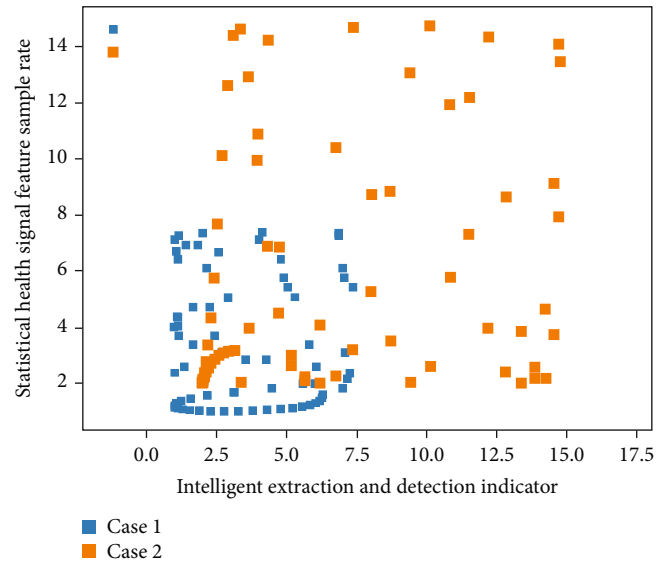

Figure 6: Intelligent health signal feature extraction and detection.

4. Application and Analysis of Health Detection System Based on Biological Signal Acquisition

4.1. Simulation Implementation of Health Detection System. The health detection system adopts a structured design idea and applies multipoint wireless connection technology. Its hardware part is composed of two parts: the LPC1769-based elderly terminal and the smart watch coordination control terminal. The LPC1769-based elderly terminal uses multichannel sensor data acquisition. Based on the LPC1769 terminal for the elderly, the data collected by various sensors is coordinated and summarized, the received data is filtered, stored, and analyzed through microprocessing, and the analyzed data is stored in the form of a wireless smart watch. It is transmitted to the designated host computer (smart watch terminal for the elderly). The data transmission process is that the wearable elderly terminal collects the temperature, pulse, and health monitoring signals of the elderly's body, respectively. After amplification and filtering by the amplifier circuit, the LPC1769 is sent to the LPC1769 for preprocessing, and the collected elderly's body is processed through multichannel sensor fusion technology.

Before the feature extraction and classification identification, it is necessary to accurately extract the active segment of the action from the SEMG and ACC signal flows collected in Figure 6. The previous active segment extraction is generally to extract the action active segment signal from the continuous signal flow.

At the same time, the introduced moving average algorithm based on SEMG signal is suitable for the extraction of isolated gestures or action segments with relatively high signal-to-noise ratio. When a system is more ordered, its information signal is lower, and vice versa. It is of great significance to introduce the concept of signal into the ACC signal representation of dynamic and static actions, which can be understood in this way; when an individual is in a static behavior, the vector amplitude of its acceleration signal can be regarded as a self-timer with a mean value of 0 after subtracting a certain mean value. In the theory of information signal, such signal has the largest uncertainty, and its signal value is the largest. When the individual is in dynamic behavior, its acceleration signal vector amplitude shows different modes with different dynamic behavior modes, and the generation of the mode is constrained by the completion process of the behavioral action.

Statistical methods such as t-test and chi-square test were used to compare the general conditions of the subjects in the management group and the control group in Figure 7. It can be seen that the average age of the management group is 68.46 ± 5.99 years old; the majority of males are 27, accounting for 54%; the living conditions are mainly couples living together, accounting for 60%, followed by living with children, accounting for 30%; education high level school or technical secondary school (36%), junior high school (28%), and primary school (22%) ranked the top three; the average age of the control group was 70.68 ± 6.83 years old; 28 women were the majority, accounting for 56%, mainly live with their children, accounting for 48%, followed by husbands and wives, 40%; primary school (26%), junior high school (24%), and illiterate (22%) are the top three; the management group and the control group are generally above average comparison of the situation, and the difference in Table 2 was not statistically significant ($P > 0.05$).

The feature vector extracted from the ACC signal of the smart watch is used to determine the specific motion trajectory information and provide guidance for whether the execution of the gesture action is a phonetic code coding action or a part code coding action: on the other hand,

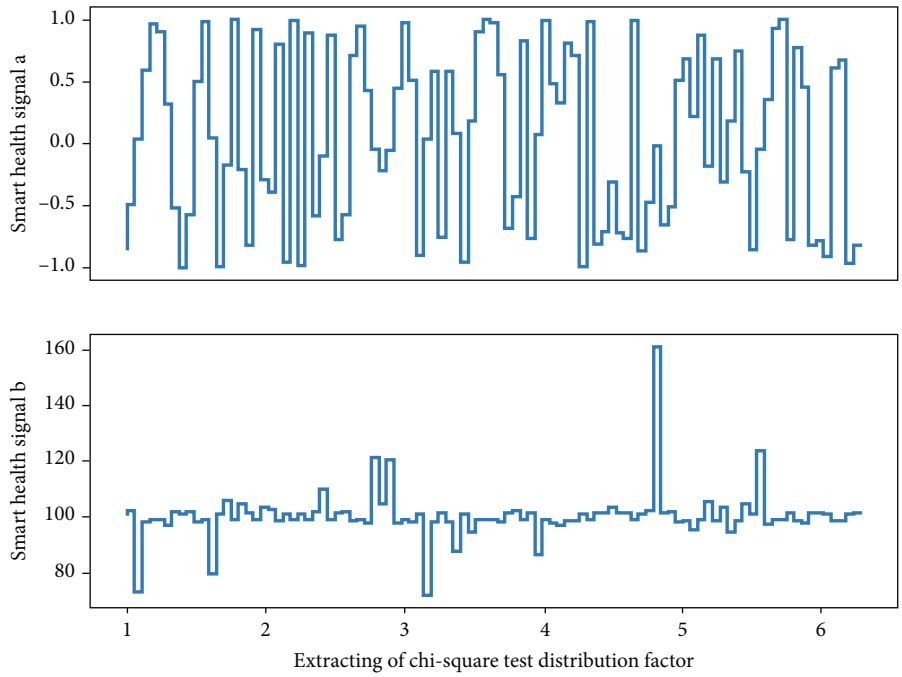

Figure 7: Chi-square test distribution of smart health signals.

Table 2: Intelligent health signal algorithm steps.

Intelligent algorithm step	Health signal texts
#include<iostream>	Signal of the smart watch
#include<fstream>	Chi-square test hrest(x, y)
Using namespace std;	Statistical $q(r-1)$ methods
Fin.open("D:/data.txt");	Were used to load case
If(!Fin)	Compare the general (q, p)
For(int i =0; i <12; i++)	Such as t-test and $m(a) - m(a-1)$
Cout<<"could not open the file" < <endl;	The control group in $y(x, t-1)$
Return -1;	Conditions of $px(q \longrightarrow p)$
Fout<<" "<<labels[i] < <endl;	Management group and $k(t) - k(t-1)$
Fout.open("D:/test.txt");	The subjects in the perber(q, p)
If(!Fout)	It is used to determine the $dy^q(x-t, t)$

the feature vector of the SEMG signal is extracted for different categories of detection indicators.

When the wearer falls, the acceleration and angular velocity in all directions will change. By setting an effective threshold, when it is judged that the acceleration vector and angular velocity vector in a certain direction exceed the threshold, it will be combined with other auxiliary information to judge whether a fall has occurred. Since the recognition of the detection indicators cannot be 100% correct, in order to reduce the transmission error, that is, a coding recognition error may lead to the recognition of the entire character error, we identify the likelihood probability sum of the four trajectories and the four detection indicators. Then, the DSP runs the ECG signal R wave identification and positioning algorithm to perform arithmetic operation on the ECG signal in the SDRAM, the result of the operation is written into the SDRAM, and a PCI interrupt is generated at the same time. The data results in the SDRAM are read back into the monitoring software of the telemedicine center, and the results are displayed on the monitor of the central server computer for reference by medical staff.

4.2. Example Application and Analysis. The health detection system randomly divided all voluntary elderly people into the management group and control group. After grouping and baseline investigation, the elderly in the management group were given special health management, while the control group did not receive special intervention for the time being. Two questionnaires were administered to the elderly in the management and control groups at baseline and after 18 months. The content of the questionnaire includes basic information of the elderly, health service utilization, health knowledge, belief, behavior, health management needs, economic burden of disease, and health utility level of the elderly. EpiData 3.1 was used for data entry, SPSS 17.0 for statistical analysis, and MATLAB 7.0 for Markov model calculation. Descriptive analysis, t-test, chi-square test, Mann–Whitney U method, multiple regression analysis, logistic regression analysis, and other statistical analysis methods were used. Since each coding action is repeatedly collected 10 times every day, the first scheme does not consider the motion trajectory information. At this time, each detection index can obtain 40 training samples per day, so that the 5-day training data folder can obtain 200 training samples. The second solution is to consider the identification of detection indicators under a specific trajectory. At this time,

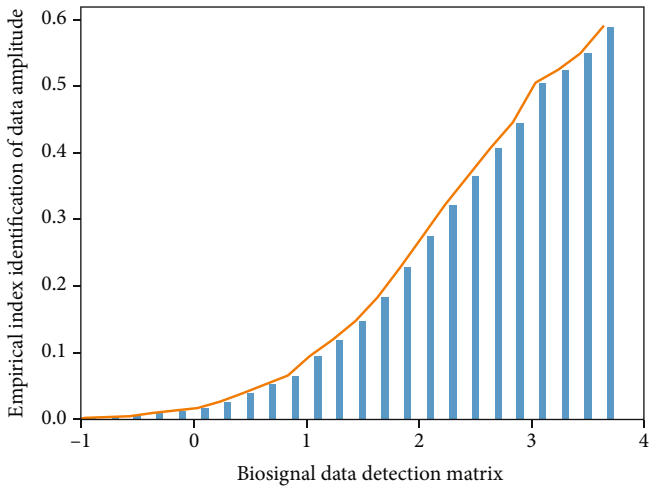

Figure 8: Identification of biosignal data detection indicators.

the number of training samples for each detection indicator provided in the training data folder every day is only 10, and a total of 50 training samples are provided in 5 days.

Figure 8 conducts health management satisfaction survey and uses the logistic regression method to conduct multivariate analysis of health management satisfaction. The results show that 97.0% of the elderly are satisfied with health management services. The difference in the impact of health status on satisfaction with health management was statistically significant ($P < 0.05$). Generally speaking, younger age groups were more satisfied, and people with diseases were more satisfied than healthy people. Those with average and poor health status were more satisfied with health management. We calculate the histogram signal and then negate it to get the histogram negative signal; here, the base of the logarithm is taken as 10, and the unit of the obtained signal value is dit. Then, we calculate the negative histogram signals successively within the moving window length.

The requirements for the number of training samples in Figure 9 for the comprehensive motion trajectory classification and recognition results are that each hand movement of each trajectory is performed for at least 4 times, and the detection index classification and recognition results require the number of training samples for each trajectory. The number of executions of each detection indicator is about 15 times. In the actual data collection process, it is ensured that each track and each detection indicator are executed no less than 15 times in multiday data collection, which greatly reduces the training burden for users. And no matter how the vocabulary changes, there are only 53 types of coding actions that need to collect training samples, and the training number of each coding action hardly changes. In software, the method of interrupt chain is adopted: suppose when the system starts, it is found that the interrupt 7 is used by the board A, and the memory area corresponding to the interrupt will be pointed to the interrupt service routine entry ISR_A corresponding to the A card; then, the system finds that the board B is also using interrupt 7, the memory area corresponding to interrupt 7 will be pointed to ISR_B, and the end of ISR_B will be pointed to ISR_A.

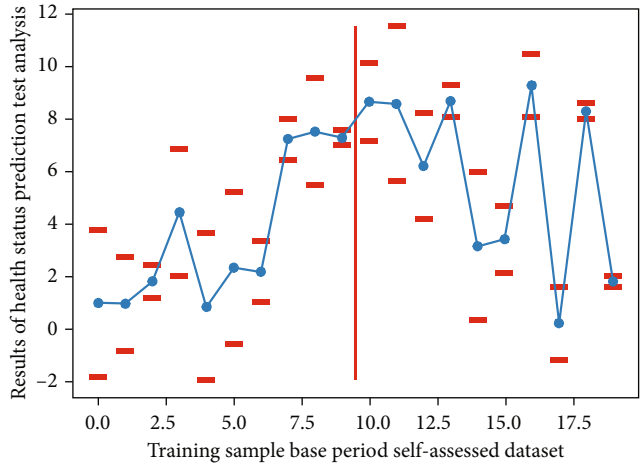

Figure 9: Self-assessed health status of training samples in the base period.

For different dynamic biosignal behaviors, the negative signal value is higher than that of static biosignal behaviors, and it maintains the same trend with the intensity and duration of dynamic biosignal behaviors. Here, Figure 10 defines that the start threshold and end threshold of active segment segmentation are equal in value. When the negative signal value is higher than the start threshold and multiple consecutive negative signal values are higher than the start threshold, it is considered to be the start of the active segment, when the negative signal value is low, the task activity segment ends when the end threshold value and subsequent consecutive negative signal values are all lower than the end threshold value. According to the description of the SNTP protocol, the performance of the synchronization source and the difference of the network path and the calibration accuracy of 1 ~ 50 ms can be provided.

The algorithm design of the threshold discrimination method is relatively simple and intuitive, and the algorithm implementation is relatively easy; so, the algorithm is widely used. However, the setting of the threshold in the algorithm

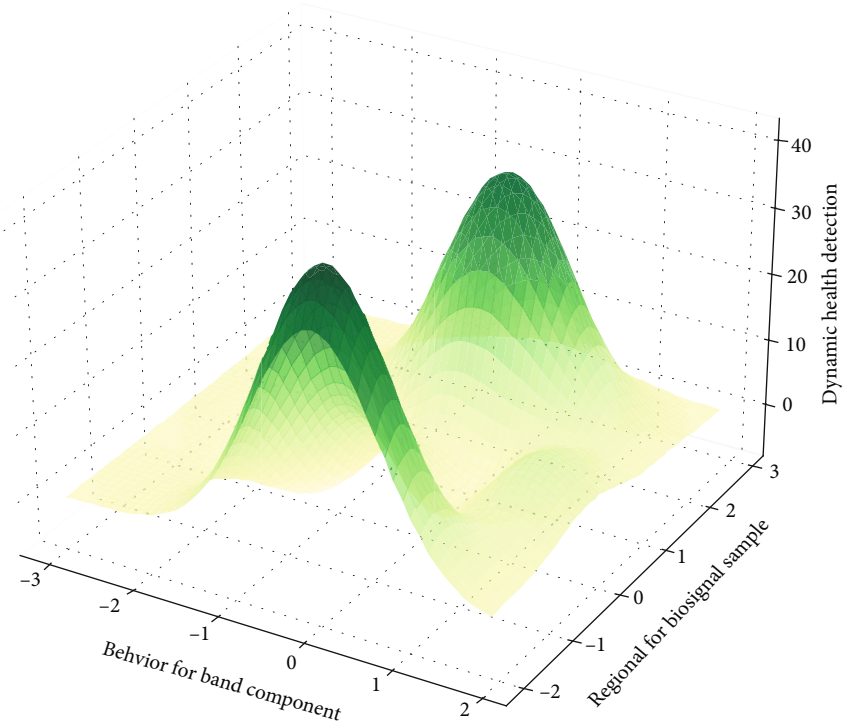

Figure 10: Dynamic biosignal behavioral health detection.

has a great influence on the accuracy of the algorithm, and the determination of the threshold should be based on a large number of experimental data. It can be seen from the experimental results that the standard deviation and coefficient of variation of the heart rate results measured by the heart rate detection algorithm used in this paper are lower than the standard deviation and coefficient of variation of the heart rate results measured by the heart rate detection algorithm that comes with Hi-watch. The stability of the heart rate detection algorithm used in this paper is better than that of the heart rate detection algorithm that comes with the Hi-watch smart watch.

5. Conclusion

This design is based on the biological signal data network with mature technology and high penetration rate and uses the smart watch as the user terminal for the elderly, which can realize remote data collection, abnormal alarm, and real-time positioning at anytime and anywhere (within network coverage). The system is based on the LPC1769 microprocessor and is composed of a pressure sensor, a temperature sensor, an MMA7455 three-axis acceleration sensor, a smart watch module, and many smart watch terminals to realize the detection of two basic medical physical parameters such as body temperature and pulse, as well as the health of the elderly and the positioning of the elderly. The delivery of emergency rescue SMS messages for the elderly. The signal collected by the sensor is processed by amplifying circuit, compensation circuit, and compensation algorithm. Its main purpose is to design a simple and more user-friendly remote medical center server-side monitoring software for users, display the multiparameter signals remotely transmitted by GPRS through the Internet on the central display in real time and accurately, and connect with the medical database at the same time. It is convenient for medical staff to manage the data. The corresponding detection algorithm is implemented on the DSP processor for physiological signals such as ECG, so that it can achieve high processing speed and accuracy, provide accurate and timely patient physiological information for medical staff, and assist medical staff to make scientific decisions. The elderly only needs to wear the wearable smart watch elderly health monitoring system on the body to realize real-time acquisition of physiological parameters. The system can also be used to find the elderly at the first time when the elderly gets lost or faint. The miniaturization, portability, and real-time nature of physiological signal acquisition of wearable smart watches will be widely used not only in elderly care but also in the medical field.

Data Availability

The data used to support the findings of this study are available from the corresponding author upon request.

Conflicts of Interest

The authors declare that they have no known competing financial interests or personal relationships that could have appeared to influence the work reported in this paper.

Acknowledgments

This work was supported by the College of Art, Shangqiu University.

References

[1] G. Şengül, M. Karakaya, S. Misra, O. O. Abayomi-Alli, and R. Damaševičius, "Deep learning based fall detection using smartwatches for healthcare applications," *Biomedical Signal Processing and Control*, vol. 71, article 103242, 2022.

[2] F. J. González-Cañete and E. Casilari, "A feasibility study of the use of smartwatches in wearable fall detection systems," *Sensors*, vol. 21, no. 6, p. 2254, 2021.

[3] C. Krittanawong, A. J. Rogers, K. W. Johnson et al., "Integration of novel monitoring devices with machine learning technology for scalable cardiovascular management," *Nature Reviews Cardiology*, vol. 18, no. 2, pp. 75–91, 2021.

[4] G. Cicirelli, R. Marani, A. Petitti, A. Milella, and T. D'Orazio, "Ambient assisted living: a review of technologies, methodologies and future perspectives for healthy aging of population," *Sensors*, vol. 21, no. 10, p. 3549, 2021.

[5] A. H. Kashou, A. M. May, and P. A. Noseworthy, "Artificial intelligence-enabled ECG: a modern lens on an old technology," *Current Cardiology Reports*, vol. 22, no. 8, pp. 6–8, 2020.

[6] J. He, J. Ou, A. He et al., "A new approach for daily life blood-pressure estimation using smart watch," *Biomedical Signal Processing and Control*, vol. 75, article 103616, 2022.

[7] M. Dörr, V. Nohturfft, N. Brasier et al., "The WATCH AF trial: smart WATCHes for detection of atrial fibrillation," *JACC: Clinical Electrophysiology*, vol. 5, no. 2, pp. 199–208, 2019.

[8] G. Biagetti, P. Crippa, L. Falaschetti, S. Orcioni, and C. Turchetti, "Human activity monitoring system based on wearable sEMG and accelerometer wireless sensor nodes," *Biomedical Engineering Online*, vol. 17, no. S1, pp. 16–18, 2018.

[9] S. Y. Lee, C. Tsou, and P. W. Huang, "Ultra-high-frequency radio-frequency-identification baseband processor design for bio-signal acquisition and wireless transmission in healthcare system," *IEEE Transactions on Consumer Electronics*, vol. 66, no. 1, pp. 77–86, 2020.

[10] M. Swapna, U. M. Viswanadhula, R. Aluvalu, V. Vardharajan, and K. Kotecha, "Bio-signals in medical applications and challenges using artificial intelligence," *Journal of Sensor and Actuator Networks*, vol. 11, no. 1, p. 17, 2022.

[11] R. Pernice, A. Parisi, S. Guarino et al., "Low invasive multisensor acquisition system for real-time monitoring of cardiovascular and respiratory parameters," in *Mediterranean Electrotechnical Conference (MELECON)*, pp. 306–310, 2020.

[12] D. Martinho, J. Carneiro, P. Novais, J. Neves, J. Corchado, and G. Marreiros, "A conceptual approach to enhance the well-being of elderly people," in *EPIA Conference on Artificial Intelligence*, pp. 50–61, 2019.

[13] Q. Lin, S. Song, I. D. Castro et al., "Wearable multiple modality bio-signal recording and processing on chip: a review," *IEEE Sensors Journal*, vol. 21, no. 2, pp. 1108–1123, 2021.

[14] C. Camara, H. Martín, P. Peris-Lopez, and M. Aldalaien, "Design and analysis of a true random number generator based on GSR signals for body sensor networks," *Sensors*, vol. 19, no. 9, p. 2033, 2019.

[15] A. Zompanti, A. Sabatini, S. Grasso et al., "Development and test of a portable ECG device with dry capacitive electrodes and driven right leg circuit," *Sensors*, vol. 21, no. 8, p. 2777, 2021.

[16] T. H. Tsai, W. Y. Lin, Y. S. Chang, P. C. Chang, and M. Y. Lee, "Technology anxiety and resistance to change behavioral study of a wearable cardiac warming system using an extended TAM for older adults," *PLoS One*, vol. 15, no. 1, article e0227270, 2020.

[17] J. Mühlsteff, W. ten Kate, A. Bonomi et al., "Systems, sensors, and devices in personal healthcare applications," in *Personalized Health Systems for Cardiovascular Disease*, pp. 51–83, Academic Press, 2022.

[18] P. Sundaravadivel, A. Fitzgerald, S. P. Mohanty, and E. Kougianos, "Easy-assist: an intelligent haptic-based affective framework for assisted living," in *Consumer Electronics (ICCE)*, pp. 3–5, 2020.

[19] G. Tamiziniyan and A. Keerthana, "Future of Healthcare: Biomedical Big Data Analysis and IoMT," in *The Internet of Medical Things (IoMT) Healthcare Transformation*, pp. 247–267, Wiley, 2022.

[20] S. Lee, Y. Chu, J. Ryu, Y. J. Park, S. Yang, and S. B. Koh, "Artificial intelligence for detection of cardiovascular-related diseases from wearable devices: a systematic review and meta-analysis," *Yonsei Medical Journal*, vol. 63, pp. S93–S107, 2022.

[21] S. Cho and S. H. Lee, "Development of smart healthcare scheduling monitoring system for elderly health care," *International Journal of Internet, Broadcasting and Communication*, vol. 10, no. 2, pp. 51–59, 2018.

[22] M. T. Mardini, Y. Iraqi, and N. Agoulmine, "A survey of healthcare monitoring systems for chronically ill patients and elderly," *Journal of Medical Systems*, vol. 43, no. 3, pp. 16–21, 2019.

[23] M. Pateraki, K. Fysarakis, V. Sakkalis et al., "Biosensors and internet of things in smart healthcare applications: challenges and opportunities," in *Wearable and Implantable Medical Devices*, pp. 25–53, Elsevier, 2020.

[24] J. O. Olmedo-Aguirre, J. Reyes-Campos, G. Alor-Hernández, I. Machorro-Cano, L. Rodríguez-Mazahua, and J. L. Sánchez-Cervantes, "Remote healthcare for elderly people using wearables: a review," *Biosensors*, vol. 12, no. 2, p. 73, 2022.